

Superconductivity near instability in MgCNi₃.

A. Ignatov, S. Y. Savrasov, T.A. Tyson

Department of Physics, New Jersey Institute of Technology, Newark, New Jersey 07102

(Dated: May 22, 2019)

To understand the role of electron-phonon interaction in superconducting MgCNi₃ we have performed density functional based linear response calculations of its lattice dynamical properties. A large coupling constant $\lambda = 1.75$ is predicted and contributing phonons are identified as displacements of Ni atoms towards octahedral interstitials of the perovskite lattice. Instabilities found for some vibrational modes emphasize the role of anharmonic effects in resolving experimental controversies.

PACS numbers: 74.25.Jb, 61.50.Ks, 74.70.Ad

The discovery of superconductivity in MgCNi₃ [1] has generated a new puzzle in the recent series of found superconductors [2]. Despite its relatively low $T_c \sim 8$ K, the presence of Ni signals the possible importance of correlation effects which makes the physics of the pairing mechanism relevant to the famous high T_c cuprates and brings the discussion of unconventional non-electron-phonon mechanism. The experimental information characterizes MgCNi₃ as moderate [1, 3] or strong [4] coupling conventional superconductor through the analysis of specific-heat data, supports the s-wave pairing by CMR experiments [5], and at the same time shows a zero-bias anomaly in tunnelling data [4] due to possible sign-changing order parameter. A clear need for detailed information about the phonon spectra emerges from these controversial data in order to clarify the role of electron-phonon interaction (EPI) and understand the mechanism of superconductivity.

In this work, we perform theoretical studies of the strength of the electron-phonon coupling in MgCNi₃ by using fully self-consistent density functional based linear response calculations [6] of the lattice dynamical properties as a function of phonon wavevector \mathbf{q} . This method was proven to provide reliable estimates for the phonon spectra and electron-phonon interactions in a large variety of systems [6, 7]. We extract a large coupling constant $\lambda = 1.75$ and identify phonons contributing to it as displacements of Ni atoms towards octahedral interstitials of the perovskite-like cubic structure. We find some of the lattice vibrations to be unstable in linear order which emphasizes the role of strong anharmonic effects in the possible resolution of the recent experimental puzzles.

The basic element of the perovskite MgCNi₃ structure is given by a carbon atom placed at the center of the cube and octahedrally coordinated by 6 Ni atoms. Our electronic structure calculation using full potential linear muffin-tin orbital (LMTO) method [8] reveals Ni-d C-p hybridized valence bands $\epsilon_{\mathbf{k}j}$ in accord with the previous studies [9, 10, 11]. The Fermi surface consists of several sheets such as rounded cube sections centered at Γ , thin jungle gym area spanning from R $[\frac{1}{2} \frac{1}{2} \frac{1}{2}] \frac{2\pi}{a}$ to M $[\frac{1}{2} \frac{1}{2} 0] \frac{2\pi}{a}$ points, dimpled square shaped hole pockets centered around X point $[\frac{1}{2} 0 0] \frac{2\pi}{a}$ as well as little ovoids

along $\Gamma - R$. The tight-binding picture discussed before [9] consists of carbon p_x , p_y , p_z orbitals hybridized with d states of three Ni atoms numerated accordingly as Ni_x, Ni_y, and Ni_z. For example (see Fig. 1) carbon p_z state hybridizes with Ni_z $d_{z^2-1^2}$ and also with Ni_x d_{xz} , Ni_y d_{yz} . Similar picture holds for carbon p_x , p_y orbitals which are not shown. As it has been noted [9], this in particular results in two antibonding states crossing the Fermi level, which in the nearest neighbor approximation have no dispersion along some directions in the Brillouin zone (BZ).

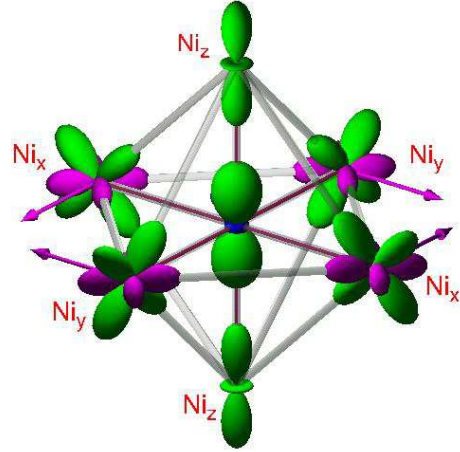


FIG. 1: Basic element of the structure and set of tight-binding orbitals relevant to low-energy physics MgCNi₃. Arrows show displacements of Ni atoms corresponding to wavevector $\mathbf{q} = [\frac{1}{2} \frac{1}{2} 0] \frac{2\pi}{a}$.

The appearance of nearly flat areas of $\epsilon_{\mathbf{k}j}$ gives rise to 2D van Hove singularity (vHS) placed 40 meV below the Fermi energy E_F which is responsible for a strong narrow peak near E_F . This has generated speculation about closeness of MgCNi₃ to ferromagnetic instability upon doping [9, 10, 11, 12]. The narrowness of the vHS band is controlled by the second-nearest neighbor hopping integrals, which for the states shown in Fig. 1 correspond to the overlap between Ni_x and Ni_y d_{xy} orbitals. As we discuss in this work, nearly unstable phonon modes

exists when each of the two Ni atoms moves toward octahedral interstitial sites. (This is shown in Fig. 1 by arrows for a phonon wave vector $\mathbf{q} = [\frac{1}{2} \frac{1}{2} 0] \frac{2\pi}{a}$). We shall see that these distortions wipe out the narrow vHS peak and give rise to a large electron-phonon coupling.

To calculate lattice dynamics of MgCNi_3 as a function of wave vector \mathbf{q} we utilize the linear response method[6, 8], We use 2κ LMTO basis set, generalized gradient approximation for exchange-correlation[13], experimental lattice constant $a=7.206$ a.u., as well as effective (40,40,40) grid in \mathbf{k} -space (total 1771 irreducible \mathbf{k} points) to generate the phonon dispersions $\omega_{\mathbf{q}\nu}$ and electron-phonon matrix elements $g_{\mathbf{k}+\mathbf{q},\mathbf{k}'\mathbf{k},\nu}$ on a (10,10,10) grid of the \mathbf{q} vectors (total 56 irreducible \mathbf{q} points).

Our calculated phonon spectrum along major high symmetry lines of the cubic Brillouin zone is given on Fig. 2. The frequencies are seen to be span up to 900 K, with some of the modes showing significant dispersion. In general, we distinguish three panels where the top three branches around 900 K are carbon based, the middle three branches around 600 K are Mg based and 9 lower branches are all Ni based. For the Γ point z-polarized modes, in particular, consist of (i) Ni_z -C against $\text{Mg}-\text{Ni}_x-\text{Ni}_y$ vibrations (186 K), (ii) pure Ni_x-Ni_y vibrations (262 K), (iii) Mg against Ni_x-Ni_y (561 K) (iv) C against Ni_z vibrations(857 K).

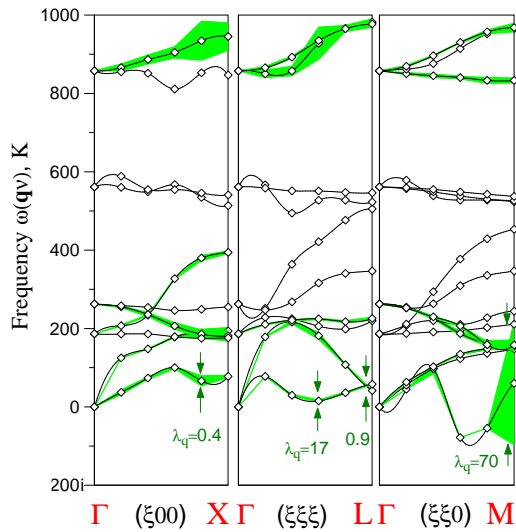


FIG. 2: Calculated phonon spectrum of MgCNi_3 using density functional linear response method. Some curves are widened proportionally to the phonon linewidths.

A striking feature of this phonon spectrum is the presence of a low-frequency acoustic mode which is very soft and is even seen to be unstable along $(\xi\xi 0)$ direction in the BZ. This mode is essentially Ni based and corresponds to perpendicular movements of two Ni atoms towards octahedral interstitials of the perovskite structure. The latter is made of each of the four Ni atoms and two

Mg atoms. For example, considering the xy plane (see Fig. 1) for the \mathbf{q} point M such movements can be seen as a 2D breathing around this vacant interstitial. We find a similar situation for other wave vectors and in other directions of the BZ, where each pair of Ni atoms prefers such in-phase displacements perpendicular to each other. The softness and instability here can be understood as the octahedral interstitials are only places to escape for each Ni atom stressed between two surrounding carbons.

The discussed displacements affect the overlap integrals between nearest Ni t_{2g} orbitals which control the width of the vHS band. For the xy plane these are the hoppings between d_{xy} orbitals (see Fig. 1). It is therefore clear that these modes should have large EPI. As they bend the Ni-C bonds, this effect has already been previously emphasized[9] in some form by considering rotations of the Ni based octahedra. However, here, we point out totally different movements where, for example, Ni_x -C and Ni_y -C bonds can be seen as changing their relative angle.

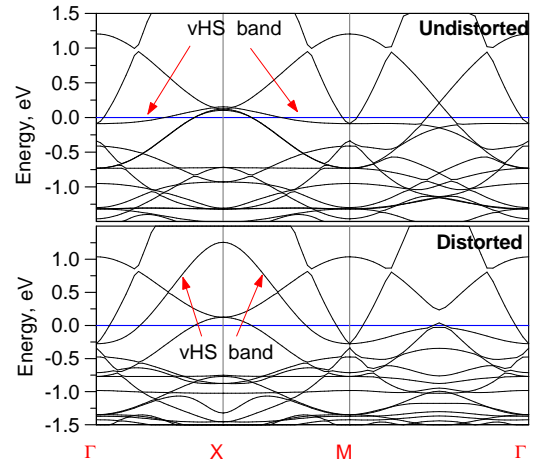


FIG. 3: Calculated one-electron structure corresponding to the Ni based frozen phonon with $\mathbf{q} = [\frac{1}{2} \frac{1}{2} 0] \frac{2\pi}{a}$. Top panel - undistorted bands, bottom panel - distorted bands corresponding to the Ni displacements by 0.2 Å.

To illustrate the crucial change in the electronic structure due to such distortions, Fig. 3 shows two one-electron spectra in the vicinity of the Fermi level corresponding to the M point frozen phonon involving Ni_x displacement along the y axis in phase with the Ni_y displacement along the x axis as illustrated on Fig. 1. The top panel of Fig. 3 corresponds to the undistorted energy bands drawn in the original cubic BZ for easier comparison with the published data [9, 10, 11]. As the point $[\frac{1}{2} \frac{1}{2} 0] \frac{2\pi}{a}$ is now a reciprocal vector of the new doubled lattice, the bands are seen to be simply folded, and the narrow vHS band is readily recognized. When we introduce a distortion by 0.2 Å, the only essential difference is the width of the vHS band which now dis-

perses as much as 1.5 eV. Given the smallness of the assumed displacement this emphasizes the large electron-phonon coupling. Its appearance cannot be understood from a simple geometric overlap between the two t_{2g} orbitals (d_{xy} states between Ni_x and Ni_y shown on Fig. 1). We therefore look for an electronic enhancement due to nesting-like features of the Fermi surface. Indeed, such nesting can be found for the two dimpled square shaped hole pockets centered at X separated exactly by the wave vector $[\frac{1}{2}\frac{1}{2}0]\frac{2\pi}{a}$. We have confirmed that feature by corresponding calculation of the integral $\sum_{\mathbf{k}jj'} \delta(\epsilon_{\mathbf{k}j} - \epsilon_F) \delta(\epsilon_{\mathbf{k}+qj} - \epsilon_F)$ which provides the total phase space available for the electrons to scatter at given wave vector \mathbf{q} with no energy change.

We now turn our discussion to the detailed dependence of the electron-phonon coupling across the entire BZ. This at least can be done for all stable phonons. Fig. 2 shows the calculated phonon linewidths $\gamma_{\mathbf{q}\nu}$ by widening some representative dispersion curves $\omega_{\mathbf{q}\nu}$ proportionally to $\gamma_{\mathbf{q}\nu}$. Each phonon linewidth is proportional to [14] $\sum_{\mathbf{k}jj'} |g_{\mathbf{k}+\mathbf{q}j'\mathbf{k}j}^{\mathbf{q}\nu}|^2 \delta(\epsilon_{\mathbf{k}j} - \epsilon_F) \delta(\epsilon_{\mathbf{k}+qj} - \epsilon_F)$ where the electron-phonon matrix element is found self-consistently from the linear response theory [6]. In particular, we see that some phonons have rather large linewidths. This, for example holds, for all carbon based higher lying vibrational modes. The strength of the coupling, $\lambda_{\mathbf{q}\nu}$, for each mode can be obtained by dividing $\gamma_{\mathbf{q}\nu}$ by $\pi N(0)\omega_{\mathbf{q}\nu}^2$, where $N(0)$ is the density of states at the Fermi level equal to 5.3 st./[eV*cell] in our calculation. Due to large $\omega_{\mathbf{q}\nu}^2$, this unfortunately results in strongly suppressed coupling for all carbon modes which would favor high critical temperatures. The coupling, however, is relatively strong for the Ni based modes. For example, we can find λ 's of the order of 1–3 for the Ni based optical phonons around 250 K. Again, the analysis of the polarization vectors shows that these vibrations involve Ni movements towards octahedral interstitials. For example, (see Fig. 1) the movement of Ni_x and Ni_y atoms along the z direction either in-phase or out-of phase result in larger overlap between Ni_z Ni_y d_{yz} orbitals and between Ni_z Ni_x d_{xz} orbitals. Similar to what we find for the M point using the frozen phonon method (Fig. 3), this again enlarges the vHS bandwidth resulting in large EPI. A extremely large coupling ($\lambda \sim 70$) occurs for the soft acoustic mode involving the interstitial breathing (M -point). Here we point out a triple effect: (i) breathing of four Ni_x Ni_y atoms into the interstitial, which results in larger d_{xy} overlap, (ii) nesting enhancement which helps wiping out the vHS peak, and, (iii) the smallness of $\omega_{\mathbf{q}\nu}^2$. As the linewidth of this particular phonon is so large, the concept of phonon itself has to be questioned, but due to a smallness of the phase space associated with this vibration, this has a little effect on integral characteristics such as λ .

Unfortunately, finding the integral value of λ is another challenging problem due to the appearance of the imag-

inary frequencies. Neglecting the unstable mode completely results in the average coupling constant equal to 0.95 mainly due to the discussed Ni vibrations around 250 K (see Fig. 2).. It is however clear that the low-frequency mode has a large contribution to λ and cannot be omitted. We have asked a question for which wave vectors \mathbf{q} this mode is unstable? Since we know its dispersion across the entire BZ, we can determine a surface in \mathbf{q} space which separates the real and imaginary frequencies. Fig. 4 shows the result of such an analysis. We see the area around the Γ point which continues along the lines towards the R , M , and X points. Here we find the stability of the mode. The area around the M point, where we find enormously large EPI, is seen to be very small . This is also clear from the dispersion relations shown on Fig. 2 for the $(\xi\xi 0)$ direction where the frequency becomes real just near the M point itself.

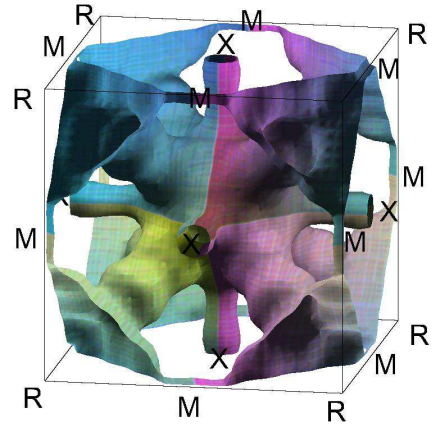


FIG. 4: Surface in the Brillouin zone which separates stable and unstable areas for the Ni based acoustic mode.

The persistence of the instability for the large portion of the BZ assumes that it is better to deal with a locally distorted structure. Unfortunately, since the instability does not occur for any of the high symmetry point, it is practically impossible to study it using the frozen phonon method. On the other hand, our recent extended x-ray absorption fine spectroscopy experiments (EXAFS) performed with MgCNi_3 samples reveal local structural distortions [15]. The experiment measures Ni-Ni correlation function and is capable determining the profile of the interatomic potential. It was found, that an anharmonic double-well-like potential exists with the depth of the order of 20K. Clearly, such a small depth on the temperature scale indicates that the distortions are dynamical and will not be seen in diffraction experiments. The curvature of the double well at the equilibrium corresponds to the imaginary frequency of 50i K. This is in accord with our linear response calculations which determined the negative second order derivatives around the equilibrium of the cubic lattice. The question arises about the spectrum of excitations of this anharmonic oscillations.

tor. Due to the smallness of the depth in the double well, we find that the ground state zero motions occur at ~ 70 K with the first excited state placed at 220 ± 20 K resulting in a first transition frequency equal to 150 K.

It is now clear that our instability is not related to a statically distorted structure of MgCNi_3 but should be resolved using an anharmonic theory of the EPI. To perform the calculation we recall a generalized expression for the coupling constant λ [16, 17] proportional to:

$$\sum_{\mathbf{k}, \mathbf{k}'j'} \sum_n \frac{(f_{\mathbf{k}j} - f_{\mathbf{k}'j'})\delta(\epsilon_{\mathbf{k}j} - \epsilon_{\mathbf{k}'j} + \omega_n)|G_{\mathbf{k}'j'\mathbf{k}j}^{(n)}|^2}{[\omega_n]^2} \quad (1)$$

where the summation over the eigenstates n of the anharmonic oscillator appears here with $\omega_n = \epsilon_n - \epsilon_0$ being the excitation frequencies around the ground state level. The generalized electron-phonon matrix element $G_{\mathbf{k}'j'\mathbf{k}j}^{(n)}$ involves transitions from the ground to all excited states and also includes changes in the effective one-electron potential to all orders with respect to the displacements. Note that this expression is converted back to the formula of the harmonic theory if one assumes $\omega_n = n\omega$ and the selection rule δ_{n1} for the matrix elements over the phonon states valid within linear response. The most important is the effect of the frequency denominator which appears in Eq. (1). As we found, the anharmonic acoustic mode has the first excitation frequency of 150 K; this has to be used for estimating the EPI. Using the well-known result that the summation over n in (1) is fastly convergent [16], leads to the values of ω_n which are still too small on the electronic energy scale. Therefore, we can safely replace the difference $f_{\mathbf{k}j} - f_{\mathbf{k}'j'}$ in (1) by the $\omega_n\delta(\epsilon_{\mathbf{k}j} - \epsilon_F)$.

To perform the estimate of λ we assume that for all wavevectors where the mode is instable, the anharmonic well exists and its excitation frequencies $\epsilon_n - \epsilon_0$ should be used according to the expression (1). We also approximate $G_{\mathbf{k}'j'\mathbf{k}j}^{(n)}$ by its linear response counterpart $\delta_{n1}g_{\mathbf{k}+\mathbf{q},j'\mathbf{k}j}^{\mathbf{q}\nu}$ which leaves $\omega_{n=1} = 150K$ in the summation over n . The approximation neglects higher order expansions of the screened potential with respect to the displacements resulting in scatterings including multi-phonon processes such as $\mathbf{k}' = \mathbf{k} \pm 2\mathbf{q}, \mathbf{k} \pm 3\mathbf{q}$. Taking them into account will in principle only increase our estimate.

Our resulting value of λ for this anharmonic mode appears to be 0.80. Adding the result for $\lambda = 0.95$ from all other modes our total λ is now 1.75. This is consistent with the values of λ extracted from specific heat measurements [1, 3, 18] and would cause MgCNi_3 to be a strong-coupling conventional superconductor. To estimate the T_c we use Allen-Dynes modified McMillan T_c expression [19] with our calculated $\omega_{\log} = 115K$. The smallness of this value reflects our result that the coupling is mainly due to the low-frequency phonon modes while our calculated average phonon frequency is 400 K.

Varying the Coulomb pseudopotential μ^* from 0.1 to 0.3 results in decreasing T_c from 15K to 7 K. The latter figure is close to the experimentally determined transition temperature, which assumes enhanced value of μ^* . Note that the same conclusion has been reached based on the recent analysis of the specific heat data [18]. As spin fluctuations may be important due to localized nature of Ni d orbitals, this result is not surprising at all. It is, for example, known [20] that for $V \mu^* = 0.3$. In fact, at the absence of spin fluctuations, μ^* is usually 0.10-0.15 and T_c in MgCNi_3 would be larger. We conclude that spin fluctuations partially suppress superconductivity, the result expected from the conventional theory. We finally note that while existing resistivity measurements are still controversial, indications exist that the electron-phonon transport spectral function $\alpha_{tr}^2 F(\omega)$ is sharply peaked at $\omega \sim 110K$ [21], i.e. precisely what we find in our work. However, strong anharmonicity may significantly alter the Bloch-Grüneisen form of the temperature dependence as it is, for example, known for the case of Pb. Clearly, more detailed transport measurements and their interpretation are required.

In conclusion, by performing density linear response calculations of the electron-phonon interaction in MgCNi_3 we reported the value of $\lambda = 1.75$ consistent with the strong-coupling limit of electron-phonon mechanism of superconductivity. The unusually large anharmonic correction to λ for the lattice near instability is emphasized which may be prompting to discover new superconductors with higher critical temperatures.

We thank W. Pickett and I. I. Mazin for useful comments. The work was supported by the grants NSF DMR No. 0238188, 9733862, 0209243, US DOE No. DE-FG02-99ER45761, NJSGC No. 02-42.

- [1] T. He *et. al.*, Nature **411**, 54 (2001).
- [2] J. Nagamatsu *et. al.*, Nature **410**, 63 (2001); S. Uji *et. al.*, Nature **410**, 908 (2001); S. S. Saxena *et. al.*, Nature **406**, 587 (2000); Matzdorf *et. al.*, Science **289**, 746 (2000).
- [3] J.-Y. Lin, *et. al.*, Phys. Rev. B **67**, 052501 (2003).
- [4] Z. Q. Mao *et. al.*, cond-mat/0105280.
- [5] P. M. Singer, *et. al.*, Phys. Rev. Lett. **87**, 257601 (2001).
- [6] S.Y. Savrasov *et. al.*, Phys. Rev. Lett. **69**, 2819 (1992); *ibid.*, **72**, 372 (1994).
- [7] S.Y. Savrasov, *et. al.*, Phys. Rev. Lett. **77**, 4430 (1996); *ibid.* **90**, 056401 (2003).
- [8] S. Y. Savrasov, Phys. Rev. B **54**, 16470 (1996).
- [9] D. J. Singh *et. al.*, Phys. Rev. B **64**, 140507(R) (2001).
- [10] S. B. Dugdale *et. al.*, Phys. Rev. B **64**, 100508(R) (2001).
- [11] J. H. Shim *et. al.*, Phys. Rev. B **64**, 180510(R) (2001).
- [12] H. Rosner *et. al.*, Phys. Rev. Lett. **88**, 027001 (2002).
- [13] J. P. Perdew *et. al.*, Phys. Rev. Lett. **77**, 3865 (1996).
- [14] P. B. Allen, Phys. Rev. B **6**, 2577 (1972).
- [15] A. Ignatov *et. al.*, Phys. Rev. B **67**, 064509 (2003).
- [16] J. C. K. Hui, P. B. Allen, J. Phys. F **4**, L42 (1974).
- [17] V. Meregalli, *et. al.* Phys. Rev. B **57**, 14453 (1998).

- [18] A. Wälte *et. al.*, cond-mat/0208364.
- [19] P. B. Allen and R. C. Dynes, Phys. Rev. B **12**, 905 (1975).
- [20] S. Y. Savrasov, *et.al.* Phys. Rev. B **54**, 16487 (1996).
- [21] T. G. Kumary, Phys. Rev. B **66**, 064510 (2002).